Limits on Hot Intracluster Gas Contributions to the Tenerife Temperature Anisotropy Map

J.A. Rubiño-Martín
Instituto de Astrofísica de Canarias
Vía Láctea s/n. 38200 La Laguna, Spain.

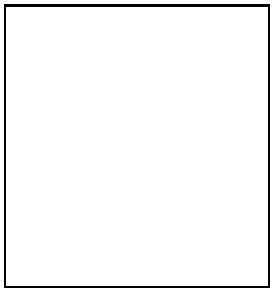

We limit the contribution of the hot intracluster gas, by means of the Sunyaev-Zel'dovich effect, to the temperature anisotropies measured by the Tenerife experiment. The data is cross-correlated with maps generated from the ACO cluster catalogue, the ROSAT PSPC catalogue of clusters of galaxies, a catalogue of superclusters and the HEAO 1 A-1 map of X-ray sources. There is no evidence of contamination by such sources at an rms level of $\sim 8\mu$K at 99% confidence level at 5^{o} angular resolution. We place an upper limit on the mean Comptonization parameter of $y \leq 1.5 \times 10^{-6}$ due to nearby structures at the same level of confidence. These limits are slightly more restrictive than those previously found by a similar analysis on the COBE / DMR data and indicate that most of the signal measured by Tenerife is cosmological.

1 Introduction

In this work we study the contribution of nearby structures on the temperature anisotropies measured by the Tenerife map (Gutiérrez et al. 2000). The Sunyaev-Zel'dovich (SZ) effect (Zel'dovich & Sunyaev, 1969) is expected to give the largest contribution to the secondary anisotropies in the CMB, and we shall center our analysis on it. We shall look for correlations between the Tenerife CMB data and template maps generated from cluster catalogues; in particular, we use the ACO (Abell, Corwin & Olowin 1989), and ROSAT PSPC catalogues (Vikhlinin et al. 1998). To test the hypothesis that the CMB signal is generated by hot diffuse gas distributed on supercluster scales we also include a supercluster catalogue (Einasto et al. 1994) in our analysis. Finally, we also constructed template maps from the HEAO 1 A-1 map of X-ray sources (Kowalski et al. 1984) that should trace the distribution of hot electrons.

2 Statistical Method.

At any given frequency, the CMB anisotropy map can be considered a superposition of contributions of cosmological origin, T_{CMB}, astrophysical origin, αM, and instrument noise, N: $T = T_{CMB} + \alpha M + N$. α is a conversion factor -to be determined- that gives the amplitude of the contribution of foreground sources to the CMB temperature anisotropies. We shall construct template maps of the temperature

anisotropies induced on the CMB spectrum by the hot gas traced by clusters. We shall name template map the term αM.

Assuming that the contribution of foreground sources is uncorrelated with the cosmological signal and noise in the temperature anisotropy map, then the cross correlation of the CMB and the template maps $C_{TM}(\theta)$ is related with the template map autocorrelation function $C_{MM}(\theta)$ as: $C_{TM}(\theta) = \alpha C_{MM}(\theta)$. A best-fit value of α is obtained by minimizing (Banday et al. 1996)

$$\chi^2 = \sum_{ij} [C_{TM}(\theta_i) - \alpha C_{MM}(\theta_i)] M_{ij}^{-1} [C_{TM}(\theta_j) - \alpha C_{MM}(\theta_j)]. \quad (1)$$

In this expression M_{ij} is the covariance matrix of the cross-correlation functions (Ganga et al. 1993) defined as follows: $M_{ij} = < [C(\theta_i) - < C(\theta_i) >][C(\theta_j) - < C(\theta_j) >] >$, with θ_i, θ_j two arbitrary angular separations in the sky. $C(\theta)$ is the cross correlation of the template map and one single realization of the observed sky. Realizations of the sky were performed in two different ways: (a) at each measured temperature we add a random realization of a gaussian distributed noise with zero mean and the variance at that point. (b) We performed Monte Carlo CMB simulations of the Tenerife data drawn from a gaussian distribution with variance $C_l = 6C_2/l(l+1)$ at each multipole, normalized to $Q_{rms-PS} = 20\mu$K. We assumed a Harrison-Zel'dovich power spectrum for the primordial fluctuations since, together with the previous normalization, is a good approximation at the scales probed by the Tenerife experiment (Gutiérrez et al. 2000). To each point in the CMB map we add a realization of the noise as in (a). In both cases, the average $< .. >$ was obtained from a thousand realizations.

The minimum-variance estimate is:

$$\hat{\alpha} = \sum_{ij} \frac{C_{MM}(\theta_i) M_{ij}^{-1} C_{TM}(\theta_j)}{\sum_{ij} C_{MM}(\theta_i) M_{ij}^{-1} C_{MM}(\theta_j)} \quad (2)$$

with formal error

$$\sigma_{\hat{\alpha}} = (\sum_{ij} C_{MM}(\theta_i) M_{ij}^{-1} C_{MM}(\theta_j))^{-1/2}. \quad (3)$$

The approach (a) described above does not include sample variance. We estimated the associated error bar by performing a thousand Monte Carlo realizations of the CMB sky and finding α from the correlation with the template maps. As expected, the average value of α was zero. The dispersion around this mean, σ_s, is a measure of both cosmic variance and the variance coming from random alignments. On the other hand, the approach (b) includes all contributions to the variance in the estimate of $\hat{\alpha}$.

3 Data and Template Maps.

The results of the Tenerife CMB experiments are presented in Gutiérrez et al. (2000). The observations were performed in two frequencies: 10 and 15 GHz covering 5000 and 6500 square degrees, respectively. The experiments are sensitive to multipoles $l = 10 - 30$ which corresponds to the Sachs-Wolfe plateau of the radiation power spectrum. The experiment uses a double-differencing technique to measure, with a 5^o FWHM beam. The maps are in the North Galactic hemisphere and have a galactic latitude $b \geq 20^o$.

Let us briefly describe the catalogues that will be used. The ACO all-sky catalogue contains 4073 rich clusters of galaxies, each having at least 30 members within magnitude range m_3 to $m_3 + 2$ (m_3 is the magnitude of the third brightest cluster member) and each with redshift less than 0.2. The HEAO 1 A-1 catalogue is essentially a catalogue of ACO clusters with X-ray emission in the energy range $0.5 - 20$keV. ROSAT is a catalogue of X-ray selected objects. It includes from poor groups till rich clusters of galaxies. These clusters were serendipitously detected in the ROSAT PSPC high Galactic latitude pointed observations ($b \geq 30^o$). The satellite covers a large energy range ($0.1 - 2$keV) in the soft X-ray band. The cluster redshifts range from $z = 0.015$ to $z > 0.5$ in the area of the sky covered by Tenerife.

The Tenerife experiment operates on the Rayleigh-Jeans regime and the effect of the hot electrons is to produce a decrement on the radiation temperature. Therefore, if the experiment has detected any contribution from hot gas, cold spots in the data and the template maps should be correlated. The anisotropy depends linearly on the central electron temperature, cluster core radius and electron density: $\delta T/T_o \propto -r_c T_e n_e$ (Zel'dovich & Sunyaev 1969).

To elaborate a template map, since clusters are unresolved by the antenna, we assign a number to each pixel: zero if there was no cluster, and a contribution proportional to the cluster SZ optical depth if there was one.

Finally, we also included in our analysis the supercluster catalogue of Einasto et al. (1994). This catalogue was elaborated from the distribution of rich clusters of galaxies up to redshift $z = 0.1$, extracted from the ACO catalogue described above. Contrary to clusters, superclusters can not be considered point-like. Therefore, different hypothesis about the gas distribution could lead to different results. As a first approximation, we took the gas distributed homogeneously on a sphere of the size of the supercluster (L). This template is very convenient in order to check Hogan (1992) hypothesis about the local origin of temperature anisotropies. We called this template "superclusters with homogeneous gas distribution". We checked that the correlation level did not depend on the gas distribution by chosing a model with a density profile
$n(r) = n_e[1 + (r/r_c)^2]^{-1}$, where $r_c \sim L/10$ is a fiducial radius. We called this template "superclusters with concentrated gas". Finally, both templates were convolved with the Tenerife beam pattern before performing the correlation analysis.

4 Numerical Results and Discussion.

Table 1 summarizes the results of our analysis. After substracting the mean and normalizing the templates to unit variance, the autocorrelations and cross correlations were computed given equal weight to each pixel.

The SZ effect will generate approximately equal and negative contributions at 10 and 15GHz. If the signal detected is real one should expect equal and positive values of α at the two frequencies. In Table 1 we give $\hat{\alpha}$, $\sigma_{\hat{\alpha}}$ as given by eqs. (2) and (3), and χ^2 per degree of freedom (dof) in the two approaches described in Sec. 2. For simplicity, we termed (a) "without sample variance" and (b) "with sample variance". In the case (a), we also give the error associated with sampling variance σ_s, which should be added in quadrature with $\sigma_{\hat{\alpha}}$. For each template we calculate the cross-correlation with the 15GHz and 10GHz maps. Since the latter covers a smaller fraction of the sky, we also correlate a reduced 15GHz map (denoted by 15c in the table) cut to the size of the 10GHz map to eliminate the bias introduced by the different sky coverage.

No significative detections (larger than 2σ) were found by either of the two methods. We always found negative values of α, i.e., cold spots in the template map correlate with hot spots in the data, contrary to what one would expect if there was a significant SZ contribution. The largest signal was obtained at the 15c ROSAT template map. Since the amplitude of the SZ effect does not change much at the Tenerife frequencies, consistency would require a fluctuation of the same order to be present at 10GHz. Furthermore, when sample variance was not included in the covariance matrix, the best-fit was never a good fit. Only when it was included χ^2/dof became of order unity. To conclude, we can only set upper limits on the value of α. Taking the results on 15GHz, we limit $\alpha \leq 0.24$ at the 99% confidence level.

For an experiment with such a beam width like Tenerife, one could not expect to find a large correlation between data and templates. For example, some clusters in the ACO catalogue have been found to produce temperature fluctuations of the order 100μK (Birkinshaw 1999). But they subtend an angular scale of few arcminutes and as a result the SZ signal is diluted by the large solid angle covered by the Tenerife beam. Still, the Tenerife data limits the contribution of nearby clusters and superclusters to be smaller than 8μK at 99% confidence level. The mean Comptonization parameter at $y = \frac{-\Delta T}{2T_o} \leq -1.5 \times 10^{-6}$ at the same level of confidence. Our results are slightly more restrictive than those previously found by Banday et al. (1996). Let us remark that y obtained above only limits the contribution due to nearby superclusters at 5^o scales, while the COBE result of Mather et al. (1994) applies to the contribution of all structures located between the last scattering surface and the observer. To conclude, this study, like previous ones based on the COBE / DMR data, indicate that most of the signal measured by Tenerife is not of extragalactic origin but cosmological.

Acknowledgments

We thank F. Atrio-Barandela and C.Hernández-Monteagudo for the help in the preparation of this talk and for useful discussions at Salamanca.

Table 1: Cross-correlation results.

	without sample variance				with sample variance		
ν / GHz	$\hat{\alpha}$	$\sigma_{\hat{\alpha}}$	σ_s	χ^2_{min}/dof	$\hat{\alpha}$	$\sigma_{\hat{\alpha}}$	χ^2_{min}/dof
ACO Clusters							
15	-0.05	0.017	0.08	17	-0.03	0.07	1.1
15c	-0.019	0.02	0.09	4	-0.03	0.1	0.3
10	-0.06	0.03	0.09	2	-0.05	0.07	0.4
SUPERCLUSTERS (concentrated gas)							
15	-0.12	0.015	0.09	13	-0.05	0.06	1.6
15c	-0.09	0.02	0.09	11	-0.05	0.07	1.4
10	-0.10	0.02	0.09	11	-0.1	0.06	1.8
SUPERCLUSTERS (homogeneously distributed gas)							
15	-0.11	0.017	0.09	12	-0.05	0.06	1.4
15c	-0.10	0.02	0.1	11	-0.06	0.07	1.3
10	-0.09	0.02	0.1	7	-0.08	0.07	1.4
HEAO 1 A-1 X-ray sources							
15	-0.018	0.016	0.07	17	-0.02	0.06	1.7
15c	-0.06	0.02	0.08	10	-0.08	0.07	1.16
10	-0.02	0.02	0.08	7	-0.014	0.06	0.9
ROSAT clusters.							
15	-0.12	0.018	0.09	11	-0.15	0.06	1.3
15c	-0.17	0.02	0.1	20	-0.19	0.07	2.1
10	-0.04	0.02	0.1	2	-0.04	0.06	0.3

References

1. Abell, G. O., Corwin, H. G. & Olowin, R. P. 1989, ApJ, 70, 1
2. Banday, A. J. et al. 1996, ApJ, 468, L85
3. Birkinshaw, M. 1999, Phys. Rep., 310, 97
4. Einasto, M. et al. 1994, MNRAS, 269, 301
5. Ganga, K., Cheng, E., Meyer, S. & Page, L. 1993, ApJ, 410, L57
6. Gutiérrez et al. 2000, ApJ, 529, 47
7. Hogan, C. J. 1992, ApJ, 398, L77
8. Kowalski, M. P., Ulmer, M. P., Cruddace, R. G. & Wood, K. S. 1984, ApJSS, 56, 403
9. Mather, J.C. et al. 1994, ApJ, 420, 439
10. Vikhlinin, A., McNamara, B. R., Forman, W., Jones, C. Quintana, H. & Hornstrup, A. 1998, ApJ, 502, 558
11. Zel'dovich, Ya. B. & Sunyaev, R. 1969, ApSS, 4, 301